

Quark Stars with the Strong Magnetic Fields: Considering Different Magnetic Field Geometries

Wei Wei¹, Xi-Wei Liu¹ and Xiao-Ping Zheng²

¹ College of Science, Huazhong Agricultural University, WuHan 430070, China;

² College of Physical Science and Technology, Central China Normal University, WuHan 430079, China

Received 2017 May 3; accepted 2017 June 15

Abstract We calculated the mass-radius relationship of quark stars with the magnetized density-dependent quark mass model in this work, considering two magnetic field geometries: a statistically isotropic, tangled field and a force-free configuration. In both cases, magnetic field produce decreases in the maximum quark star mass. Furthermore, tangled, isotropic magnetic field has a relatively smaller impact on the mass and radius, comparing to the force-free configuration, which imply that the geometry of interior magnetic field is at least as important as the field strength themselves when the influence of the strong magnetic field on the mass and radius is assessed.

Key words: stars: neutron — equation of state — magnetic fields

1 INTRODUCTION

Neutron star, one of the densest objects in the universe, is an important probe for the theories of extreme physics. Since the density in the interior of neutron stars is up to the ground state density of atomic nuclei by far, neutron stars are probably composed of pure quark matter or quark matter enveloped by nuclear crusts, called quark stars. Different quark matter models can be tested by calculating the structure of the quark stars and comparing them with observations. In particular, observations of the neutron stars with very high masses are useful. If each set of the models predicts a maximum mass lower than the observations, which model will be excluded. For example, the observations of $1.97 \pm 0.04M_{\odot}$ pulsar and $2.01 \pm 0.04M_{\odot}$ pulsar (Demorest et al. 2010; Antoniadis et al. 2013) have been used to significantly constrain the viable quark star models.

Quark stars are not only extremely dense, but also associated with strong magnetic fields, which estimated surface value is typically $\sim 10^{12} - 10^{13}G$. Meanwhile a few rotating radio transients and X-ray dim isolated neutron stars have been observed with even higher magnetic fields (Popov et al. 2006). Further, Soft gamma-ray repeaters and anomalous X-ray pulsars have been reported with the highest magnetic field in the neutron stars by using a unified model of magnetars to explain their observed features (Duncan and Thompson 1992; Paczynnsdi 1992;Thompson and Duncan 1995; Melatos 1999). Various observations of magnetars indicate the surface magnetic field value of $\sim 10^{15}G$, and a catalog of 26 known magnetars has been presented recently (Olausen and Kaspi 2014).

As the quark stars with strong magnetic fields appear to exist in nature, many works have been done on the properties of magnetized strange quark matter(MSQM) with various phenomenological confinement models. The significant effect of a strong magnetic field on the equation of state(EOS) of the quark matter, described by the conventional MIT bag model, had been found by Chakrabarty(1996).

The quasiparticle model, in which the effective quark mass varies with environment, was successfully used by many researchers to probe the dense MSQM(Wen et al. 2012).The special properties of MSQM with the Nambu-Jona-Lasinio model were investigated, too(Frolov et al. 2010, Fayazbakhsh & Sadooghi 2011).

Another alternative description of the SQM is called density-dependent quark mass model(DDQM), in which quark mass is dependent on the baryon density that is treated as the description of the confinement of the SQM(Plumber et al. 1984). The DDQM is stiffer than the other models, because the variation of quark mass with density is effectively equivalent to the inclusion of the first-order QCD coupling correction along with confinement. The quark stars described by the DDQM model with strong magnetic fields were studied by Anand et al.(2000).

However, one is attempted to ask how the magnetic field geometry affect the structure of the quark stars, besides magnetic field strength. The purpose of this work is to probe the effect of the magnetic field geometry on the mass-radius distribution of the quark stars, with the consideration of two different field configurations: a statistically isotropic, tangled field and a force-free configuration(Kamiab et al. 2015). The paper is arranged as following. Section 2 is devoted to the EOS of the MQSM. The M-R relations with the isotropic magnetic field and the force-free one are described in section 3 and 4, respectively. Section 5 presents our conclusions.

2 EQUATION OF STATE OF MAGNETIZED STRANGE QUARK MATTER

Here the DDQM model calculated by Anand et al.(2000) is employed to describe the EOS of MSQM. We treat SQM as a free Fermi gas of u , d , s quarks and electrons, in which the mass of each quark is parameterized as

$$m_u = m_d = \frac{C}{3n_B} \quad \text{and} \quad m_s = m_{s0} + \frac{C}{3n_B}. \quad (1)$$

Here C is a constant, n_B is the baryon number density of the quark matter and m_{s0} is the strange quark current mass. The ranges of these parameters are constrained by the stability conditions (Benevenuto 1998, Wei & Zheng 2012).

Considering the u , d , s , e system in the presence of a magnetic field B directed along the z -axis, the energy of a charged particle is given by(Landau & Lifshitz 1980)

$$\epsilon_i^\pm = [m_i^2 + p_{z,i}^2 + q_i B(2n + s + 1)]^{1/2}, \quad (2)$$

where $+$ ($-$) refer to spin-up(-down) states of the particle, m_i and q_i are mass and charge of the particle, and p_z is the momentum along the z -axis. The thermodynamic potential of the particle is as follows.

$$\begin{aligned} \Omega = \sum_i \Omega_i = & -\sum_i \frac{g_i q_i B}{2\pi^2} \sum_n (2 - \delta_{n0}) \\ & \times \int dp_z \ln[1 - e^{-\beta(\epsilon_i - \mu_i)}] - \frac{8}{45} \pi^2 T^4. \end{aligned} \quad (3)$$

The last term is the contribution of gluons, $i = (u, d, s, e)$, $g = 6$ for (u, d, s) and 2 for electron. The pressure P_i , the energy density ϵ_i , and the baryon number density n_i are obtained:

$$\begin{aligned} P_i = \frac{g_i q_i B}{2\pi^2} \sum_{n=0}^{n_{max}} (2 - \delta_{n0}) \times & \left\{ \frac{1}{2} \mu_i k_{fi} - (m_i^2 + 2nq_i B + \frac{2m_i c}{3\rho_B}) \right. \\ & \left. \times \ln\left[\frac{\mu_i + k_{fi}}{(m_i^2 + 2nq_i B)^{1/2}}\right] \right\}, \end{aligned} \quad (4)$$

$$\begin{aligned} \epsilon_i = \frac{g_i q_i B}{2\pi^2} \sum_{n=0}^{n_{max}} (2 - \delta_{n0}) \times & \left\{ \frac{1}{2} \mu_i k_{fi} + \frac{1}{2} (m_i^2 + 2nq_i B + \frac{2m_i c}{3\rho_B}) \right. \\ & \left. \times \ln\left[\frac{\mu_i + k_{fi}}{(m_i^2 + 2nq_i B)^{1/2}}\right] \right\}, \end{aligned} \quad (5)$$

and

$$n_i = \frac{g_i q_i B}{2\pi^2} \sum_{n=0}^{n_{max}} (2 - \delta_{n0}) k_{fi}, \quad (6)$$

where

$$k_{fi} = (\mu_i^2 - m_i^2 - 2n_i B)^{1/2}, \quad (7)$$

and

$$n_{max} = \text{int}[(\mu_i^2 - m_i^2)/2q_i B]. \quad (8)$$

The values $C = 75 \text{ MeV fm}^{-3}$ and $m_{s0} = 140 \text{ MeV}$ are used in the following calculations. The pressure and energy density are now generally functions of the matter density and magnetic field strength.

The primary process responsible for the amplification of the magnetic field is believed to be dynamos driven by differential rotation and convection, which produce a tangled magnetic field inside the neutron star (Duncan and Thompson 1992; Thompson and Duncan 1993). Various studies suggest that the dynamos naturally saturate at locally equipartition magnetic field strength during the initial formation of the proto-magnetar after the supernova explosion, while different layers of the remaining stellar core condense to form the neutron star (Chevalier 2005; Naso et al. 2008). Making a handful of simplified assumptions and regarding the outcome of the dynamo process (Kamiab 2015), we expect

$$\epsilon_B \propto \epsilon_g, \quad (9)$$

where ϵ_g and ϵ_B are the local energy density of the gas and the magnetic field, respectively. Since $P_g \approx \epsilon_g/3$ at this time, this immediately implies

$$\beta \frac{B^2}{8\pi} = P_g, \quad (10)$$

where β is the standard proportionality factor relating the gas and the magnetic pressure.

This relation naturally provides a profile of the magnetic field that is proportional to the pressure of the matter. Given a global value of β , we may identify a unique magnetic pressure at each density. For simplicity, we assume spherical symmetry throughout this work and β to remain fixed during the proto-magnetar's formation, following the quenching of the dynamos. Equations (1)-(10) enable us to compute the pressure, energy density, and baryon number density with the consideration of the beta equilibrium and electric charge neutrality. Examples of the EOS with different values of β are shown in Figure 1.

3 M-R RELATIONS WITH AN ISOTROPIC MAGNETIC FIELD

Choosing the unique EOS of the MSQM (as seen in Figure 1), and assuming spherical symmetry and isotropy, the M-R relations are obtained by solving the Tolman-Oppenheimer-Volkoff equations:

$$\frac{dP}{dr} = -\frac{G}{r^2} \left[\epsilon + \frac{P}{c^2} \right] \left[M + 4\pi r^3 \frac{P}{c^2} \right] \left[1 - \frac{2GM}{c^2 r} \right]^{-1}. \quad (11)$$

In addition to the modification of the EOS of the quark matter, the strong interior magnetic field may produce magnetic stress directly. Assuming that the outcome of the dynamo process is a small-scale, tangled field, which is weakly uncorrelated with the generating currents, the resulting stress may be completely described by a magnetic pressure, which is given by $P_B = (1/3)(B^2/8\pi)$. The energy density of the magnetic field is given by $\epsilon_B = B^2/8\pi$, where B is fixed by the choice of β . Smaller values of β are associated with higher values of magnetic field strength in the quark stars.

The total pressure and energy density are

$$P = P_g + P_B, \epsilon = \epsilon_g + \epsilon_B, \quad (12)$$

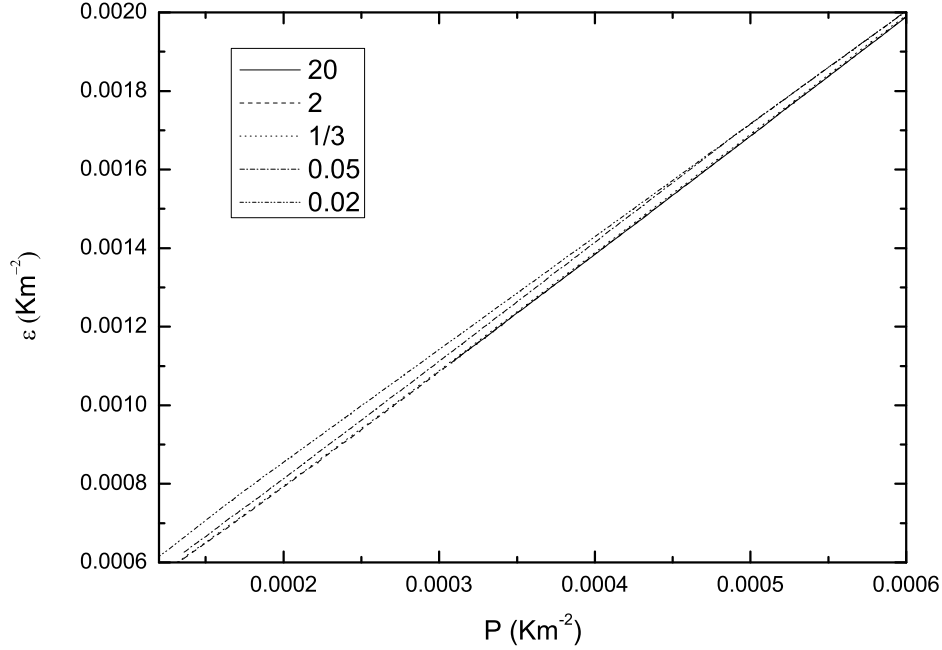


Fig. 1 Pressure(P) versus energy density (ϵ) for different values of the magnetic field strength(B) with different values of β . Smaller values of β are associated with higher values of the magnetic field strength.

where P_g and ϵ_g are pressure and energy density of the gas, here the magnetic field provides hydrostatic support for the star by entering globally in the Einstein equations. Figure 2 shows the $M - R$ relations with different magnetic field strengths by using different values of β . The mass and radius of the quark stars decrease with the effect of the magnetic fields, and larger magnetic field strengths are associated with smaller quark star maximum mass and radius. According to Equation(10), $\beta = 1/3$ corresponds to the quark star with equal pressure of the magnetic field and matter. In this condition, we get a maximum mass 6.6 percent smaller than the one without the magnetic field.

Figure 3 displays the magnetic field strengths in the center of different mass quark stars with different values of β . The central magnetic field strength is around $10^{13}G$, when the quark star's mass reach the maximum, which is reasonable according to the understanding of the magnetic fields of the neutron stars.

To illustrate the effect of the magnetic field strength on the maximum mass and radius of the quark star, Figure 4 and Figure 5 show the maximum mass and radius as functions of $1/\beta$, respectively. These relative changes are well fit by

$$\frac{\Delta M_{max}}{M_{max}} \simeq 0.081\beta^{-0.177}, \quad (13)$$

$$\frac{\Delta R_{max}}{R_{max}} \simeq 0.063\beta^{-0.136}, \quad (14)$$

for an isotropic tangled magnetic field distribution.

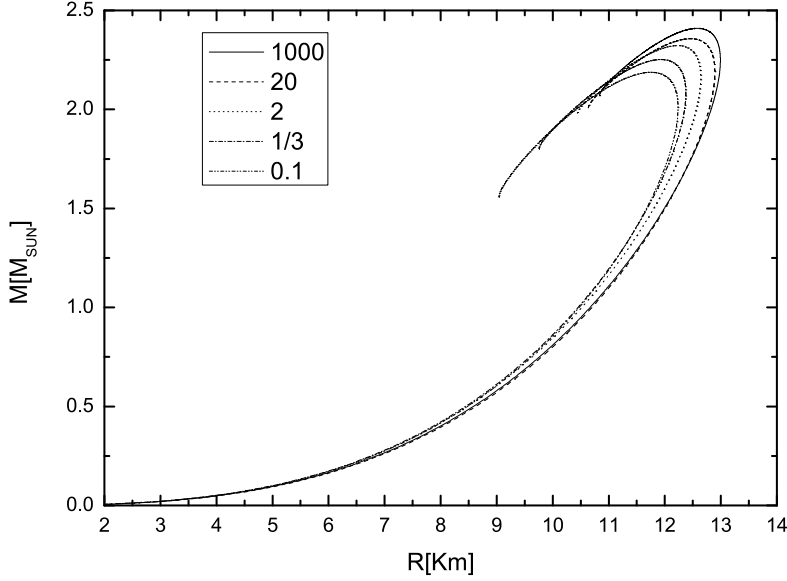


Fig. 2 The mass-radius relation for the magnetized EOS with an isotropic magnetic field. The calculation has been done for different values of β in Equation (10).

4 M-R RELATIONS WITH A FORCE-FREE MAGNETIC FIELD

Despite the small-scale, turbulent field is believed to be produced by the dynamos initially, the final magnetic field configuration remains unclear. In this paper, the magnetic field geometry: a force free configuration is considered too. After the dynamos quenching and before the formation of a crust, the quark star will reconfigure the magnetic field geometry via bulk fluid motions, resulting in a linked, nearly force-free geometry that is decided by the initial magnetic helicity (Braithwaite & Spruit 2004,2006). This is a natural consequence of the helicity conservation, corresponding to the minimum energy state at fixed magnetic helicity (Broderick & Narayan 2008). To assess the effect of the force-free condition on the hydrostatic equilibrium of the star, we need to solve Newtonian Euler equation and impose static conditions. According to the results of Kamiab et al.(2015), in dimensions where $G = 1$ and $c = 1$, the Euler equation coming from $\nabla_\nu T_{gas}^{\mu\nu} = 0$ is given by

$$\frac{dP_g}{dr} = -(\epsilon_g + P_g)g, \quad (15)$$

where g is

$$g \equiv \frac{M + 4\pi(P_g + P_B^{(r)})r^3}{r^2(1 - 2M/r)}. \quad (16)$$

Using $P_B^{(r)} = \frac{1-2\Delta}{3} \frac{\langle B^2 \rangle}{8\pi}$ and the equipartition assumption, the total radial pressure becomes

$$P_g + P_B^{(r)} = \left(1 + \frac{1-2\Delta}{2\beta}\right)P_g. \quad (17)$$

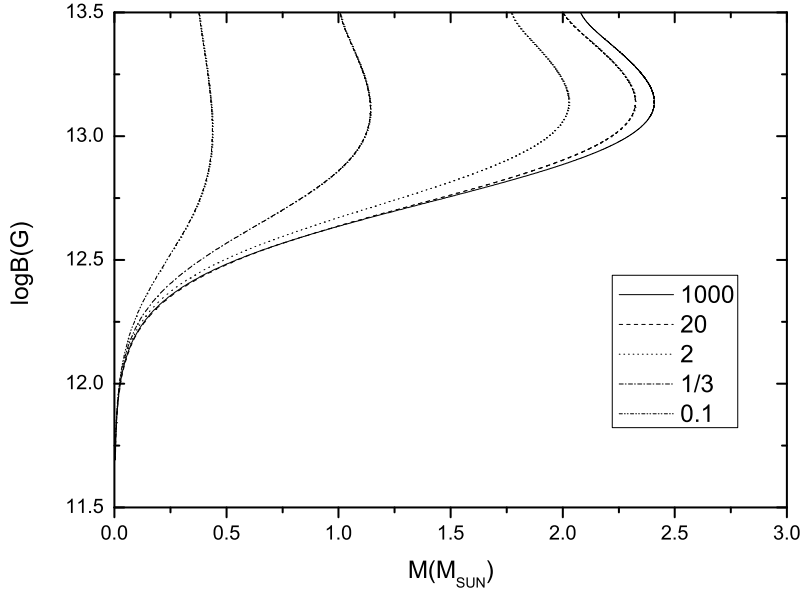


Fig. 3 The central magnetic field strengths in different mass quark stars with different β values.

Δ is an anisotropy parameter that quantifies the anisotropy of this average configuration. An anisotropy parameter $\Delta = -1$ corresponds to a purely tangential magnetic field configuration and $\Delta = 2$ corresponds to a purely radial field. An isotropic average field will have $\Delta = 0$. We refer to the isotropic core with $\Delta = 0$ in a range of radii from 0 to 3km.

Using the EOS of DDQM model(Figure 1) and Equations (15)-(17), the resulting mass-radius relationships from numerical integration are shown in Figure 6, in which the results based on the isotropic magnetic field are also plotted for comparison.

In contrast to the case of the tangled, isotropic magnetic field, the force-free configuration produces a more obvious decrease in the maximum mass with the same value of β . The smaller the β is, the stronger the magnetic field is, and the more the difference of the maximum mass between the two configurations is.

Figure 7 explicates the central magnetic field strengths of the quark stars with a force-free configuration. The central magnetic field strength is around $10^{13}G$ when the quark star's mass reach the maximum, which is similar to the isotropic case. As before, the changes in mass and radius are well fit by the power law functions,

$$\frac{\Delta M_{max}}{M_{max}} \simeq 0.28\beta^{-0.893}, \quad (18)$$

$$\frac{\Delta R_{max}}{R_{max}} \simeq 0.11\beta^{-0.61}, \quad (19)$$

which are illustrated in Figure8 and Figure9.

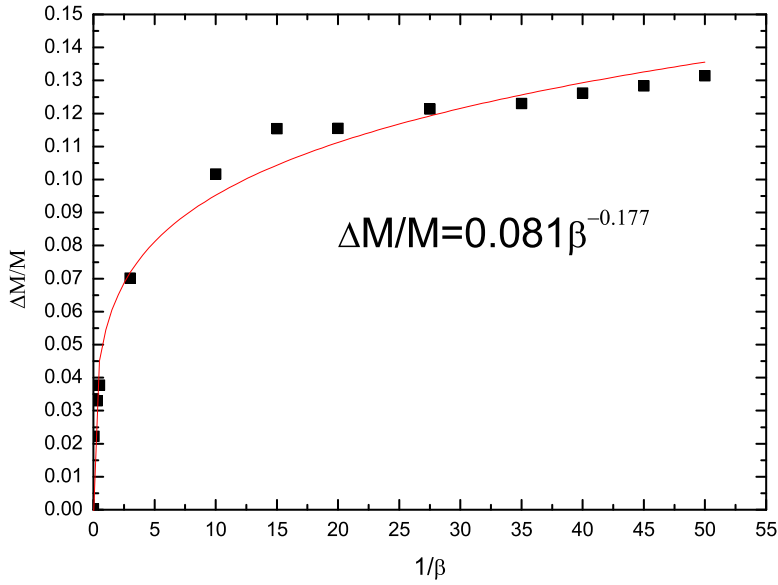


Fig. 4 Change in maximum mass of the quark star as a function of $1/\beta$ for the mass-radius relation shown in Figure 2

5 CONCLUSIONS

In this paper, we have shown that the assumed geometry of the magnetic field in the quark star is at least as important as the field strength itself, when the impact of the magnetic field on mass and radius is assessed. Both the tangled, isotropic magnetic configuration and force-free one produce decreases in the maximum quark star mass. Furthermore, tangled, isotropic magnetic field has a smaller impact on the mass, comparing to the force-free configuration.

Although the magnetic configurations reduce the maximum mass obviously, the calculations in this study indicate that the quark stars described by the DDQM model are compatible with the observations of massive neutron stars with mass $\geq 2M_{sun}$. Nevertheless, these results challenge the assertion that magnetic fields provide a means to reconcile the recent observations of very massive neutron stars with relatively soft EOS of the quark matter, whose calculated maximum mass is otherwise precluded. Some EOS of the quark matter, such as MIT bag model and quark quasi-particle model, support values of maximum mass is lower than $1.6M_{sun}$. Although many works found that the effect of the strong interactions, such as one-gluon exchange or color-superconductivity can stiffen EOS of the quark matter, strong magnetic fields change the structure of the quark stars and reduce the massive mass inversely, which bring difficulties to explain the astronomical observations of the massive neutron stars.

An interesting possibility is that the relation between the change of massive mass and internal magnetic field strength (Figs.4-5,8-9) may provide a new way to distinguish the internal magnetic field configuration (isotropic v.s. force free) or to probe the dense matter (nucleon v.s. quark) in the neutron stars. Different neutron stars might have dynamos with varying efficiency during their formation processes. Future observations of M-R relationship of the neutron stars may exhibit a more intrinsic scatter related to the internal magnetic field. Now the magnetic field in the interior of neutron stars cannot be directly measured, which is generally estimated by using the Virial theorem. If the internal magnetic

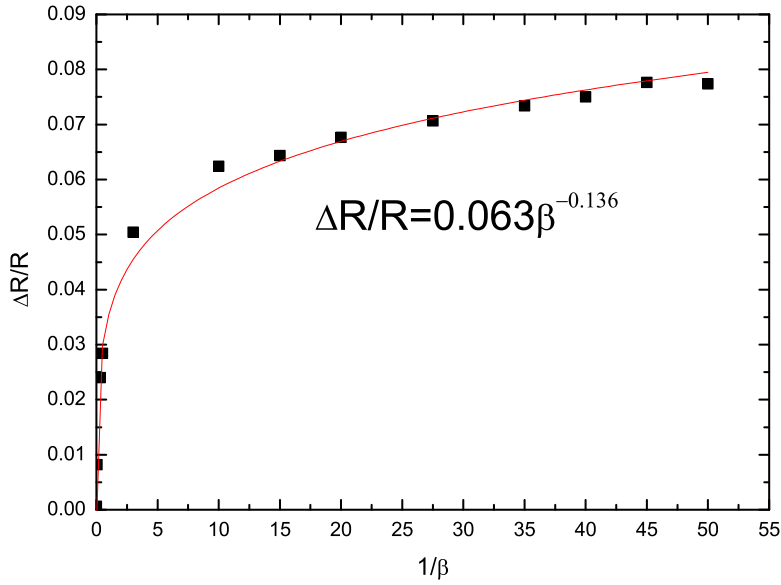


Fig. 5 Change in radius of the quark star as a function of $1/\beta$ for the mass-radius relation shown in Figure 2

field can be measured in the future, which could correlate with this scatter and provide the sign of the correlation, these will be indicative of the field configuration and dense matter in the neutron stars.

Acknowledgements This work was funded by the National Natural Science Foundation of China (NSFC) under No.11547021, No.11347108 and No.11003005.

References

- Anand, J.D., Chandrika, N., Gupta, V.K., & Singh, S. 2000, APJ, 538, 870
 Antoniadis, J., Freire, C.C., Wex, N., et al. 2013, Science, 340, 448
 Benevenuto, O.G. & Lugones, G. 1998, Int.J.Mod.Phys., D7, 29
 Braithwaite 2004] Braithwaite, J. & Spruit, H.C. 2004, Nature, 431, 819
 Braithwaite 2004] Braithwaite, J. & Spruit, H.C. 2006, A&A, 450, 1097
 Broderick, A.E. & Narayan, R. 2008, MNRAS, 383, 943
 Chakrabarty, S. 1996, Phys.Rev.D, 54, 1306
 Chevalier, R.A. 2005, APJ, 619, 839
 Demorest, P.B., Pennucci, T., Ransom, S.M., et al. 2010, Nature, 467, 1081
 Duncan, R.C., Thompson, C. 1992, ApJ, 392, L9.
 Fayazbakhsh, S. & Sadooghi, N. 2011, Phys.Rev.D, 83, 025026
 Frolov, I.E., Zhukovsky, V.C. & Klimenko, K.G. 2010, Phys.Rev.D, 82, 076002
 Kamiab, F., Broderick, A.E. & Afshordi, N. 2015, Physics, arXiv:1503.03898
 Landau, L.D. & Lifshitz, E.M. 1980, Quantum Mechanics (New York: Pergamon)

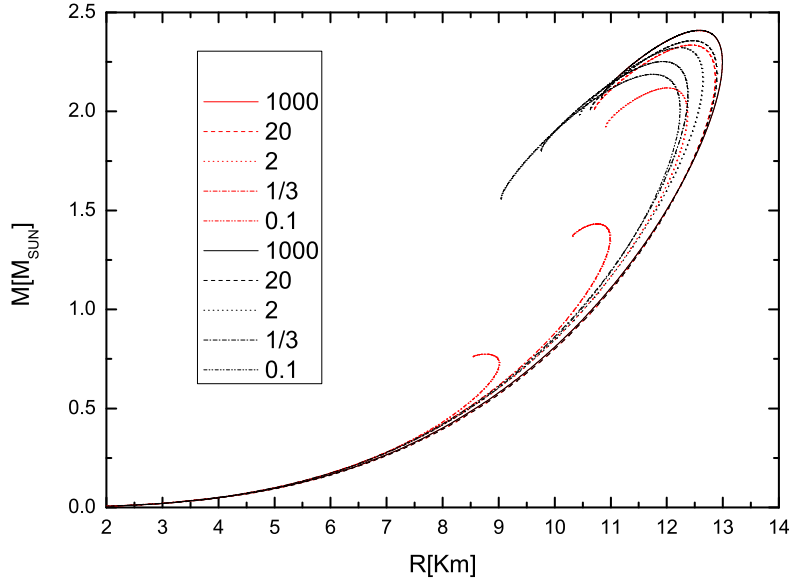


Fig. 6 The mass-radius relation for the MSQM. The red curves are for a force-free configuration magnetic field and the black curves correspond to the isotropic one.

- Melatos, A. 1999, *ApJ* 519, L77
 Naso, L., Rezzolla, L. et al. 2008, *A&A*, 479, 167
 Olausen, S.A. & Kaspi, V.M. 2014, *ApJS* 212, 6,
 Paczynski, B. 1992, *Acta Astron.*, 42, 145
 Plumber, M. et al. 1984, *Phys.Lett.B*, 139, 198
 Popov, S.B, Turolla, R., Possenti, A. 2006, *MNRAS*, 369, L23
 Thompson, C. & Duncan, R.C. 1995, *MNRAS*, 275, 255
 Thompson, C. & Duncan, R.C. 1996, *ApJ*, 473, 322
 Thompson, C. & Duncan, R.C. 1993, *ApJ*, 408, 194
 Wei, W. & Zheng, X.P. 2012, *Astroparticle Physics*, 37, 1
 Wen, X.T., Su, S.Z., Yang, D.H., et al. 2012, *Phys.Rev.D*, 86, 034006

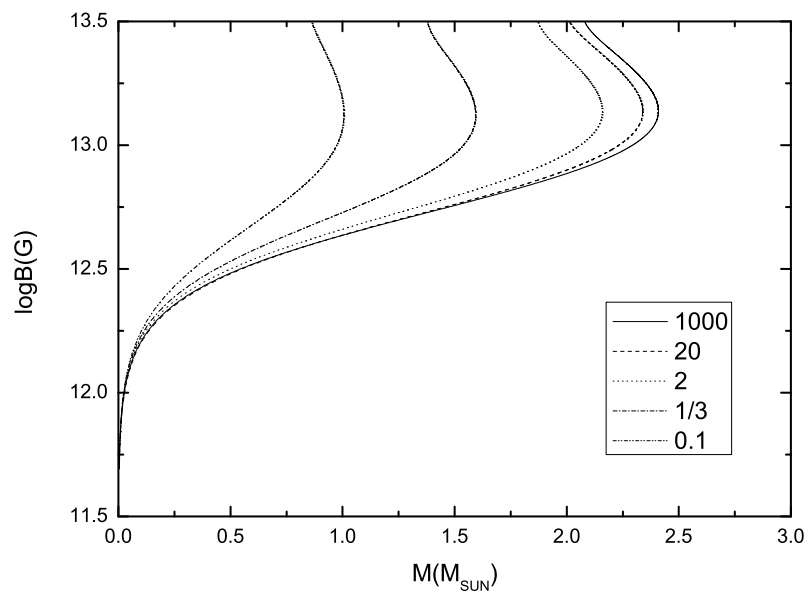


Fig. 7 The central magnetic field strengths in different mass quark stars with different β values.

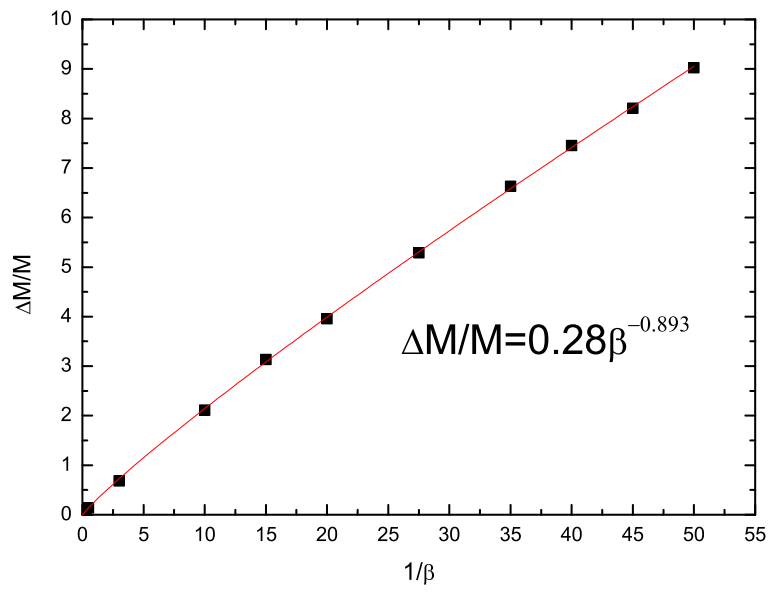


Fig. 8 Change in maximum mass of the quark star as a function of $1/\beta$ for the force-free configuration magnetic field

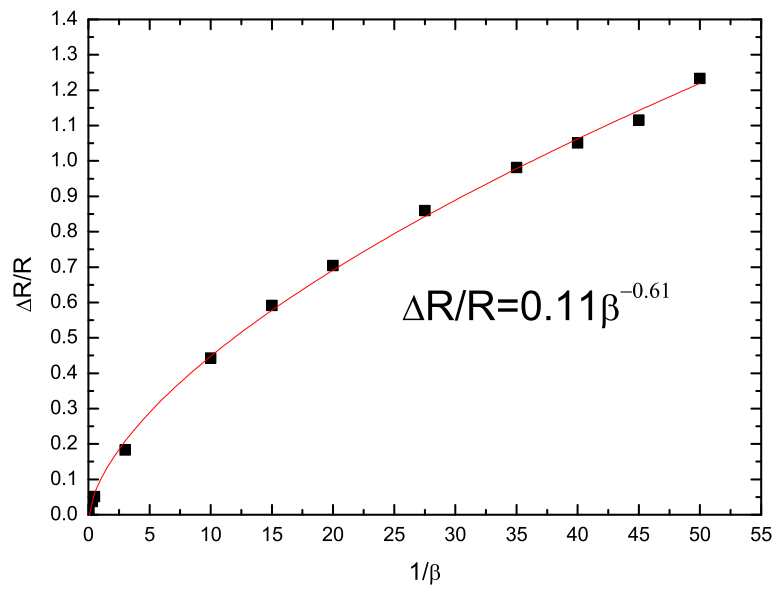


Fig. 9 Change in radius of the quark star as a function of $1/\beta$ for the force-free configuration magnetic field